Decrepitation Model For Capacity Loss During Cycling of Alloys in Rechargeable Electrochemical Systems

R.A. Huggins* and W.D. Nix**

*Faculty of Engineering, Christian-Albrechts University, D-24143 Kiel, Germany
**Department of Materials Science and Engineering, Stanford University, Stanford, CA 94305, U.S.A.

Abstract. Mechanisms that are involved in the loss of capacity upon the cycling of electrochemical cells are discussed. The inherent instability of the electrochemical interface and the resultant geometrical changes are characteristic of electrodes in which the reactant is a pure element. On the other hand, decrepitation can play an important role in the case of polyphase electrodes in which significant changes in specific volume occur. A simple one-dimensional model is presented that shows the mechanism and the important parameters that are involved in particle fracture. It predicts that decrepitation will lead to a terminal particle size, as is found experimentally.

1. Introduction

One of the important issues in the practical use of electrochemical cells is their behavior under cycling conditions. A common observation is that the capacity falls as a function of the number of charge-discharge cycles. Reduced performance upon cycling is found in almost all of the common battery systems. There are a number of possible reasons for this problem, and not all systems exhibit the same behavior.

This is generally known to be a special problem in some systems that employ metal hydrides as the negative electrode reactant, and can also be particularly acute in lithium systems when either pure lithium or lithium alloys are used as negative electrode reactants in ambient temperature cells. The mechanisms responsible for this behavior are very different in cases in which pure elemental electrodes are used from those in which the electrode reactants undergo phase transformaations with appreciable volume changes.

2. Problems of Interface Stability on Cycling of Pure Metals

In order to achieve good rechargability, a consistent electrode geometry must be maintained on both the macroscopic and microscopic scales. However, a microscopically flat interface is inherently unstable during the recharging of a pure metal electrode, even in the case of a chemically clean surface. This process involves electrodeposition, and it has been shown that there can be an electrochemical analog of the constitutional supercooling of liquid alloys that occurs ahead of a growth interface during thermally-driven solidification [1,2].

This will be the case if the current density is such that solute depletion in the electrolyte near the electrode surface causes the local gradient of the element's chemical potential in the electrolyte immediately adjacent to the solid surface to be positive. Under such a condition there will be a tendency for any protuberance upon the surface to grow at a faster rate than the rest of the interface. This leads to exaggerated surface roughness, and eventually to the formation of either dendrites or filaments. In more extreme cases, it leads to

the nucleation of solid particles in the liquid electrolyte ahead of the growing solid interface.

The protuberances upon a clean growing interface can grow far ahead of the general interface, often developing into dendrites. A general characteristic of dendrites is a tree-and-branches type of morphology, which has very distinct geometric and crystallographic characteristics, due to the orientation dependence of either the surface energy or the growth velocity.

A different phenomenon that is often mistakenly confused with dendrite formation is related to the fact that the electrolytes that are commonly used in lithium cells are not stable at the very negative potentials that are present at high lithium activities. It has been shown from thermodynamic arguments that this is an unavoidable inherent problem when using electrolytes containing organic cationic groups, regardless of whether the electrolyte is an organic liquid or a polymer [3].

The result is the formation of a reaction product layer on the electrode surface. This layer is typically an ionic conductor, so that electrodeposition on the underlying interface can take place by ionic transport through it. The term solid electrolyte interphase (SEI) was introduced some time ago to describe such layers [4].

Such layers often have defects in their structure or thin spots that can lead to variations in their impedance. Regions of higher current lead to locally faster deposition and the formation of filamentary growths upon the electrode surface.

When such a filament, sometimes called a whisker, grows ahead of the main interface the protective reaction product layer on its tip will typically be locally less thick. This means that the local impedance to the passage of ionic current is further reduced, resulting in a higher current density and more rapid growth in that location. This behavior can be exaggerated if the reaction product layer is somewhat soluble in the electrolyte, with a greater solubility at elevated temperatures. When this is the case, the higher local current leads to a higher local temperature, and a greater solubility. The result is then a locally thinner blocking layer, and an even higher local current.

Furthermore, the current distribution near the tip of a protrusion that is well ahead of the main interface deve-

lops a 3-dimensional character, leading to even faster growth than the main electrode surface, where the mass transport is essentially 1-dimensional. In relatively low concentration solutions, this leads to a runaway type of process, so that the protrusions consume most of the solute, and grow farther and farther ahead of the main, or bulk, interface.

This phenomenon results in the metal deposit on the electrode having a hairy or spongy character. During a subsequent discharge step, the filaments often get disconnected from the underlying metal, so that they cannot participate in the electrochemical reaction, and the rechargeable capacity of the electrode is reduced. This electronically disconnected and non-recyclable lithium is sometimes called dead lithium.

The electrolyte decomposition reactions are exothermic and cause local heating. Thus the instability of smooth interfaces and the formation of reaction product layers upon an ever-increasing deposit surface area can lead to thermal runaway and serious safety problems. Discussions of these interfacial instability phenomena and safety issues can be found in several places [5,6].

3. Phenomena Found in Alloys

Primarily because of these problems, elemental lithium electrodes are no longer used in rechargeable lithium batteries today. Instead, negative electrode reactants are typically lithium-carbon or other lithium alloys. Reviews of the work in this area are available in a number of places [7-11].

An entirely different type of phenomenon can occur in alloy electrodes. This involves the reduction of the capacity due to processes other than growth-related changes in the interfacial morphology. Instead, particles of reactant material fracture into smaller pieces, and often lose electronic contact with each other. This phenomenon is called decrepitation.

Decrepitation has long been recognized as occurring in some electrochemical systems in which metal hydrides are employed as negative electrode reactants. These are now very commonly used as energy sources in portable electronic devices, and metal hydride/nickel cells are gradually taking over this market from cadmium/nickel cells. There are two general reasons for

this. Metal hydride cells can store more energy per unit volume, and they do not cause environmental problems.

This can be a striking, and sometimes disastrous, phenomenon, for it is not specifically related to fine particles. Indeed, some bulk solid materials can also be caused to fracture, and even converted to powders by exposure to hydrogen gas if they form metal hydrides under the particular thermodynamic conditions present. This is different from the hydrogen embrittlement problem.

Similar phenomena also occur in lithium systems employing alloy electrodes. Because of its possible use in rechargeable cells, a considerable amount of attention has been given recently to the Li-Sn system, for example. The phase diagram of this systems shows that there are six intermediate phases. The thermodynamic and kinetic properties of the different phases in this system were investigated some time ago at elevated temperatures [12,13], and also at ambient temperatures [14-16]. The volume changes that occur in connection with phase

Table 1. Volume and Density of Phases in the Lithium-Tin System.

Phase	Volume per Sn Atom (A^3)	Density (g/cm^3)
Sn	34.2	5.76
LiSn	41.1	5.07
Li_7Sn_3	61.2	3.66
Li_5Sn_2	64.3	3.51
$Li_{13}Sn_5$	65.5	3.47
Li_7Sn_2	80.3	2.96
$Li_{22}Sn_5$	96.7	2.56

changes in this alloy system are large, as can be seen from the data in Table 1.

Although it is recognized that decrepitation seems to occur when reactions take place that involve large changes in specific volume, the mechanism by which this process occurs is not yet fully understood. There are, however, several empirical observations that provide some additional information.

Fracture of macroscopic materials and a decrease in the particle size of finely divided solids are generally not found as the result of phase transformations if the difference in specific volume between the two phases is not very large. This is what is found in martensitic transformations in steels and the formation of titanium hydrides. The alpha/ beta phase transformation in the palladium hydride system involves a difference is specific volume of about 10 %, and fracture does not occur under hydrogen pressure cycling conditions. On the other hand, it has been found [17] that the mechanical hardness is increased greatly by cycling. This means that the strains resulting from the phase transformation cause the generation of large concentrations of dislocations, rather than the initiation of fracture. This is an interesting type of chemically-driven strain hardening that does not involve macroscopic shape changes.

When metal hydrides that undergo larger volume changes are cycled, either in electrochemical cells or simply in contact with hydrogen gas, cracking of large objects and particle fracture often result. However, this process does not continue indefinitely. Instead, it is found that there is a terminal particle size that is characteristic of a particular material.

Experiments on lithium alloy electrodes have shown that the electrochemical cycling behavior is significantly improved if the initial particle size is already very small [18].

Compositional factors can also be important. For example, work at Sanyo Electric Co. has shown that the cycle life of lithium cells with Li-Al negative electrodes can be greatly improved by alloying [19,20]. This electrode operates by the isothermal transformation of Al into LiAl by reaction with Li. When used in a particular type of commercial cell, they found that the cycle life could be increased by more than a factor of three by alloying the aluminum with Mn or Cr, which form intermediate phases with aluminum at relatively low concentrations and can provide second phase particle hardening. Other alloying elements were found to be less effective. Solid solution alloying does not have such large effects.

4. Possible Mechanism

A satisfactory mechanistic explanation for these effects has not been presented to date. It is simply not enough to say that the observed changes in the electrochemical

capacity are due to the large volume changes involved in the electrochemically-driven reactions that take place in the electrode microstructures.

A change in specific volume will, of course, cause local rearrangements and result in mechanical stresses in adjacent parts of an electrode. This may produce a loss of electronic contact to some of the nearby particles. However, it is difficult to see how such mechanical distortions can cause particle size reduction, even if they do not occur homogeneously and concurrently in all parts of an electrode's microstructure. Particle size reduction must be the result of particle fracture processes. It is the purpose of this short note to suggest a way to look at this problem.

If it occurs uniformly, simple swelling or dilation of a solid does not generate internal stresses, and cannot cause fracture. This is what would occur if a homophase insertion reaction were to take place, instead of a polyphase reconstitution reaction that involves the nucleation and growth of a new phase. If the insertion of guest species into the host crystal structure of a particle occurs at a rate that is sufficiently slow relative to the diffusional processes that tend to make the composition spatially uniform, expansion would be uniform, and no internal stresses ensue.

Decrepitation must involve a heterogeneous process in which the growing phase has a different specific volume from that of the parent phase. Although actual particles can have a variety of shapes, we shall consider a simple one dimensional model in order to see the major features that are involved.

5. A Simple One-Dimensional Model of Decrepitation

Consider a bilayer plate structure with initial thickness $h_1 + h_2$ in which the top layer, of thickness h_1, is subjected to three-dimensional swelling through a transformation strain, and the other side is subjected to internal tensile stresses and possible fracture. This is illustrated in Fig. 1.

The following analysis of this problem is based on an approach that has been used previously to treat stresses and strains in thin films on substrates [21,22]. The particular problem discussed here is similar to an epitaxial thin film on a compliant substrate, in that the stresses generated in the film, the top layer, are sufficient to elastically strain the substrate, the bottom layer, in both extension and bending. We follow the methods that have been used to analyze this general type of film/substrate problem [23,24].

If the swelling, or larger-specific-volume, layer were detached from the rest of the plate it would be free to swell without any constraints. Let $e_T = \Delta V/V$ be the dilatation associated with solute incorporation and the formation of this larger-specific-volume phase in the absence of such constraints. For the thin film geometry this leads to an in-plane, stress-free, misfit strain
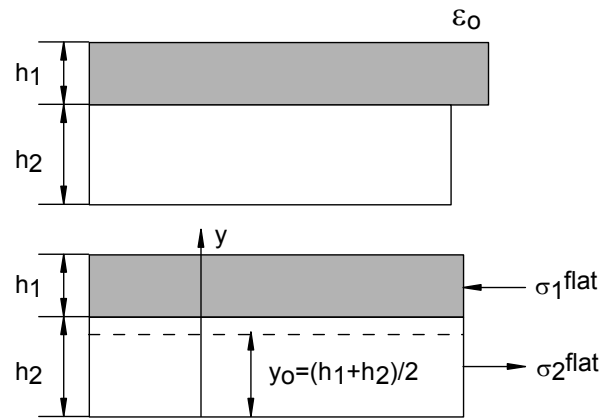

Fig. 1. Geometric relations in the simple one-dimensional bilayer model.

$$\varepsilon_0 = e_T / 3, \qquad (1)$$

as illustrated in Fig. 1. Forcing the two layers to remain mechanically compatible during the swelling process produces residual stresses in both layers, compression in the transformed larger-specific-volume layer and tension in the other layer. We wish to estimate the average tensile stress in the bottom layer and determine if it is sufficient to cause it to fracture.

If the layers are constrained to remain flat but are force-free at the edges, compatibility of the two layers leads to elastic strains ε_1^{flat} and ε_2^{flat} in both layers, as given by

$$\varepsilon_1^{flat} + \varepsilon_0 = \varepsilon_2^{flat}. \qquad (2)$$

If no in-plane forces are acting at the edges of the structure then the corresponding in-plane stresses are determined by

$$\sigma_1^{flat} h_1 + \sigma_2^{flat} h_2 = 0.,$$

so that

$$\sigma_1^{flat} = -\frac{h_2}{h_1} \sigma_2^{flat} . \tag{3}$$

Taking B to be the biaxial elastic modulus of the material, Eq. (2) may be expressed as

$$\sigma_1^{flat} + B\varepsilon_0 = \sigma_2^{flat} . \tag{4}$$

Solving Eqs. (3) and (4) leads to

$$\sigma_1^{flat} = -B\varepsilon_0 \frac{h_2}{h_1 + h_2},$$
$$\sigma_2^{flat} = B\varepsilon_0 \frac{h_1}{h_1 + h_2},$$

(5)

as the in-plane stresses in the two layers when the structure is constrained to remain flat. The tensile stresses in the low-specific-volume layer are directly proportional to the fraction of the total structure occupied by the higher-specific-volume phase.

We now wish to estimate the bending stresses that develop when the structure is allowed to bend freely. These stresses can be found by first computing the edge moment (per unit length) needed to hold the structure flat

$$M' = \int_0^{h_2} \sigma_2^{flat} (y - y_0) dy + \int_{h_2}^{h_1 + h_2} \sigma_1^{flat} (y - y_0) dy,$$

where $y_0 = (h_1 + h_2)/2$. This leads to

$$M' = -\frac{1}{2} B\varepsilon_0 h_1 h_2 .$$

The bending stresses develop when an opposite edge bending moment (per unit length)

$$M = -M' = \frac{1}{2} B\varepsilon_0 h_1 h_2 , \tag{6}$$

is applied to the structure. A simple plate bending relation gives

$$\sigma^{bend} = \frac{12M}{(h_1 + h_2)^3} (y - y_0) ,$$

which with Eq. (6) leads to

$$\sigma^{bend} = -\frac{3B\varepsilon_0 h_1 h_2 (h_1 + h_2 - 2y)}{(h_1 + h_2)^3} . \tag{7}$$

Finally, the average bending stress in the layer under tension is

$$\overline{\sigma}_2^{bend} = \frac{1}{h_2} \int_0^{h_2} \sigma^{bend} dy ,$$

which with Eq. (7) becomes

$$\overline{\sigma}_2^{bend} = -\frac{3B\varepsilon_0 h_1^2 h_2}{(h_1 + h_2)^3} . \tag{8}$$

Then the total average stress in this layer is found by adding Eqs. (5) and (8):

$$\overline{\sigma}_2 = \sigma_2^{flat} + \overline{\sigma}_2^{flat}$$

or

$$\overline{\sigma}_2 = B\varepsilon_0 \frac{h_1 (h_1^2 - h_1 h_2 + h_2^2)}{(h_1 + h_2)^3} \tag{9}$$

Taking $h = h_1 + h_2$ and defining $h_2 = \alpha h$, the stress in the layer may be expressed as

$$\overline{\sigma}_2 = B\varepsilon_0 (1 - \alpha)(1 - 3\alpha + 3\alpha^2) . \tag{10}$$

By using the definition of α and comparing Eqs. (5) and (10) we see that the effect of the bending stresses is to reduce the tensile stresses in the low-specific-volume phase by the factor $(1 - 3\alpha + 3\alpha^2)$.

6. Fracture Analysis

We now wish to investigate the conditions under which tensile stresses in the lower-specific-volume plate of thickness h_2 may lead to fracture. We will assume that fracture occurs when the tensile stress reaches the well-known Griffith-Irwin relation,

$$\sigma_{fracture} = \frac{K_{Ic}}{\sqrt{\pi c}},$$

where K_{Ic} is the fracture toughness of the material and c is the flaw size. We follow the approach taken in the study of cracking of thin films on substrates and take the flaw size to be equal to the thickness of the layer under tension. Thus the fracture stress may be expressed as

$$\sigma_{fracture} = \frac{K_{Ic}}{\sqrt{\pi h_2}} = \frac{K_{Ic}}{\sqrt{\pi h}} \frac{1}{\sqrt{\alpha}}. \qquad (11)$$

We now assume that fracture of this layer will occur whenever the stress $\bar{\sigma}_2$ exceeds the fracture stress $\sigma_{fracture}$. Alternatively, the conditions for fracture are satisfied when

$$\frac{\bar{\sigma}_2}{\sigma_{fracture}} > 1.$$

Using Eqs. (10) and (11) this fracture condition can be expressed as

$$\frac{B\varepsilon_0 \sqrt{\pi h}}{K_{Ic}} f(\alpha) > 1, \qquad (12)$$

where

$$f(\alpha) = \sqrt{\alpha}(1-\alpha)(1-3\alpha+3\alpha^2). \qquad (13)$$

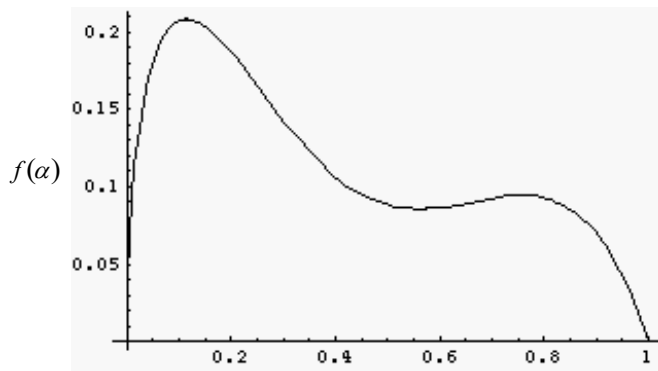Figure 2 shows how $f(\alpha)$ varies with α, the fraction of the total thickness.

Fig. 2. Variation of the parameter $f(\alpha)$ with the fraction transformed.

We note that $f(\alpha) = 0$ both at $\alpha = 1$. where the larger-specific-volume transformed layer is infinitesimally thin and no significant stresses are generated in the underlying layer, and when $\alpha = 0$, where the flaw size

tends to zero. Thus fracture will not occur at these limits. The function $f(\alpha)$ reaches a maximum value of 0.2085 at $\alpha = 0.1124$. This corresponds to the maximum driving force required for fracture. By setting $f(\alpha) = 0.2085$ we may use Eq. (12) to find the critical size below which fracture will not occur for any thickness of the transformed phase. This leads to a critical size of

$$h_c \approx \frac{23}{\pi}\left(\frac{K_{Ic}}{B\varepsilon_0}\right)^2 = \frac{23}{\pi}\left(\frac{3K_{Ic}}{Be_T}\right)^2.$$
(14)

7. Estimating the Terminal Particle Size

Using this simplified model and Eq. (14), we can make a rough estimate of the terminal size for particles in an electrode. Values of the fracture toughness can range from 3 MPa$\sqrt{m}$ for very brittle ceramics to 30 MPa$\sqrt{m}$ for very tough metals, where m is meters (length). The value of the biaxial modulus B is also material-dependent. The strain parameter e_T depends upon the crystallographic information for the phases involved.
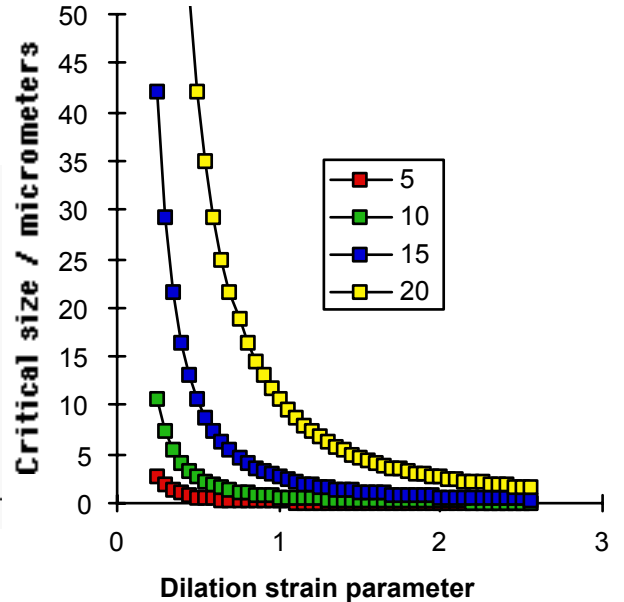

Fig. 3. Influence of the dilation strain parameter upon the critical size below which fracture will not occur for materials with different values of fracture toughness, expressed in MPa$\sqrt{m}$.

Figure 3 shows how the critical size varies with the value of the strain parameter e_T for different values of the fracture toughness, assuming that B is 100 GPa. Although based upon a simple one-dimensional model, it is seen that fracture will continue to occur until the characteristic dimension becomes very small if the change in volume resulting from the phase transformation is large for modest values of the fracture toughness. In the case of Li-Sn alloys the total transformation strain e_T is 1.83. Assuming a fracture toughness of 10 MPa$\sqrt{m}$, this value would be about 0.2 micrometers.

8. Summary

There are several mechanisms that can play significant roles in the deterioration of the capacity of electrochemical cells under cycling conditions. Interface stability problems are paramount when the electrode reactant is a pure element. On the other hand, decrepitation can be important when heterogeneous polyphase reactions take place in which significant changes occur in the specific volume of electrode materials.

A simple one-dimensional model has been presented which allows the calculation of the conditions under which fracture will be caused to occur in a two-phase structure due to specific volume mismatch. This model predicts that there will be a terminal particle size below which further fracture will not occur. The value of this characteristic dimension is material-specific, depending upon the magnitude of the volume mismatch and the fracture toughness of the lower-specific-volume phase.

9. References

[1] R.A. Huggins, J. Electrochem. Soc. **122**, 90C (1975).

[2] R.A. Huggins, and D. Elwell, J. Crystal Growth **37**, 159 (1977).

[3] G. Deublein and R.A. Huggins, Solid State Ionics **18/19**, 1110 (1986).

[4] E. Peled, J. Electrochem. Soc. **126**, 2047 (1979).

[5] J. Yamaki, in: Lithium Ion Batteries, (M. Wakihara and O. Yamamoto, Eds.) Wiley-VCH, ,1998, p. 67.

[6] U. von Sacken, E. Nodwell, and J.R. Dahn, Solid State Ionics **69**, 284 (1994).

[7] R.A. Huggins, in: Space Electrochemical Research and Technology, NASA Conference Publication 2484 (1987), p. 179.

[8] R.A. Huggins, J. Power Sources **26**, 109 (1989).

[9] R.A. Huggins, in: Fast Ion Transport in Solids, (B.Scrosati, A. Magistris, C.M. Mari and G. Mariotto, Eds.) Kluwer Academic Publishers, 1992, p. 143.

[10] R.A. Huggins, J. Power Sources **81-82**, 13 (1999).

[11] R.A. Huggins, in: Handbook of Battery Materials, (J.O. Besenhard, Ed.) Wiley-VCH, 1999, p. 359.

[12] C.J. Wen and R.A. Huggins, J. Solid State Chem. **35**, 376 (1980).

[13] C.J. Wen and R.A. Huggins, J. Electrochem. Soc. **128**, 1181 (1981).

[14] J. Wang, I.D. Raistrick and R.A. Huggins, J. Electrochem. Soc. **133**, 457 (1986).

[15] A. Anani, S. Crouch-Baker and R.A. Huggins, in: Proc. Symp. on Lithium Batteries, (A.N. Dey, Ed.) Electrochem.Soc., 1987, p. 365.

[16] A. Anani, S. Crouch-Baker and R.A. Huggins, J. Electrochem. Soc. **134**, 3098 (1987).

[17] J.A. Ferrante and R.A. Huggins, unpublished results (1989).

[18] J. Yang, M. Winter and J.O. Besenhard, Solid State Ionics **90**, 281 (1996).

[19] T. Nohma, S. Yoshimura, K. Nishio and T. Saito, in: Lithium Batteries; New Materials, Developments and Perspectives, (G. Pistoia, Ed.) Elsevier, 1994, p. 417.

[20] K. Nishio and N. Furukawa, in: Handbook of Battery Materials, (J.O. Besenhard, Ed.) Wiley-VCH, 1999, p. 19.

[21] W.D. Nix, "Mechanical Properties of Thin Films", Metall. Trans. **20A**, 2217 (1989).

[22] S.P. Baker and W.D. Nix, "Mechanical Properties of Thin Films on Substrates", in: Optical Thin Films III: New Developments, Proc. SPIE, **1323**, 263-276 (1990).

[23] L.B. Freund and W.D. Nix, "A Critical Thickness Condition for a Strained Compliant Substrate/Epitaxial Film System" Applied Physics Letters **69**, 173-175 (1996).

[24] L.B. Freund, J.A. Floro, E. Chason, "Extensions of the Stoney formula for substrate curvature to configurations with thin substrates or large deformations" Applied Physics Letters **74**, 1987-1989 (1999).